

## Supplementary information

# Microwave Synthesis and Gas Sorption of Calcium and Strontium Frameworks

Chun-Ting Yeh,<sup>a</sup> Wei-Cheng Lin,<sup>a</sup> Sheng-Han Lo,<sup>a</sup> Ching-Che Kao,<sup>a</sup> Chia-Her Lin,\*<sup>a</sup> and Chun-Chuen Yang<sup>b</sup>

<sup>a</sup>Department of Chemistry, Chung-Yuan Christian University, Chungli 32023, Taiwan. Fax: +886-3-2653399; Tel: +886-3-2653315; E-mail: chiahher@cycu.edu.tw

<sup>b</sup>Department of Physics, Chung-Yuan Christian University, Chungli 32023, Taiwan.

Figure S1. Powder X-ray diffraction patterns with varied temperatures for **CYCU-1**.

Figure S2. Powder X-ray diffraction patterns under vacuum and varied temperatures for **CYCU-1**.

Figure S3. Observed and fitted X-ray powder diffraction patterns for **CYCU-1**.

Figure S4. Powder X-ray diffraction patterns with varied temperatures for **CYCU-2**.

Figure S5. Powder X-ray diffraction patterns under vacuum and varied temperatures for **CYCU-2**.

Figure S6. Observed and fitted X-ray powder diffraction patterns for **CYCU-2**.

Figure S7. FT-IR spectra.

Figure S8. UV-vis absorption spectra.

Figure S9. Photoluminescence emission spectra.

Figure S10. Powder X-ray diffraction patterns after N<sub>2</sub> sorption.

Figure S11. The pore size distributions.

Figure S12. The CO<sub>2</sub> adsorption isotherms at 195 K and 273 K for **CYCU-1**.

Figure S13. Isosteric heat of adsorption for CO<sub>2</sub> in **CYCU-1**

**Table S1.** Selected bond lengths.

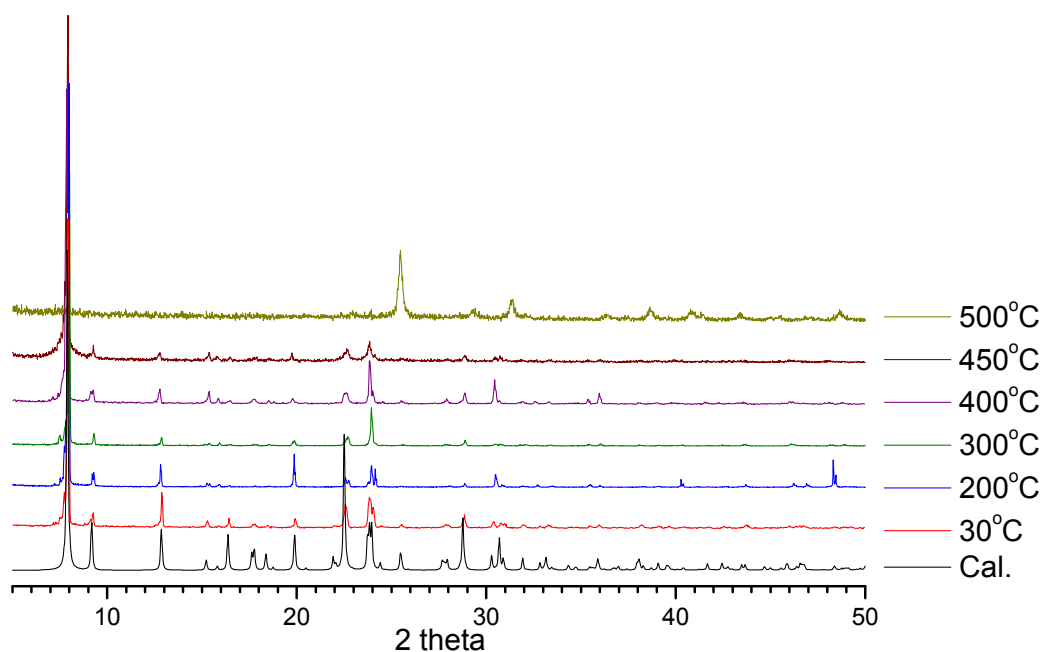


Figure S1. Powder X-ray diffraction patterns with varied temperatures for **CYCU-1**.

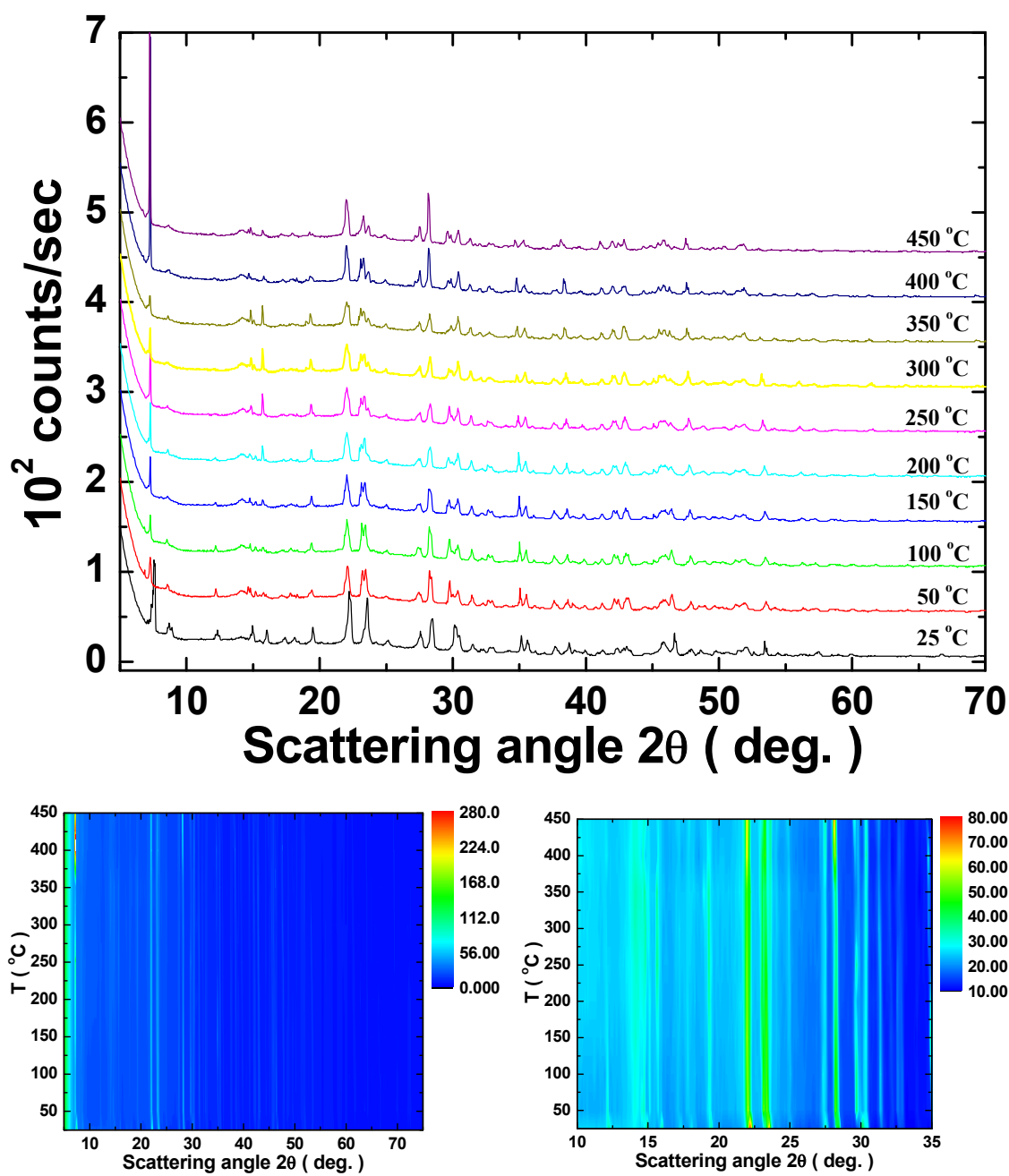


Figure S2. Powder X-ray diffraction patterns under vacuum ( $1 \times 10^{-4}$  torr) and varied temperatures for **CYCU-1**.

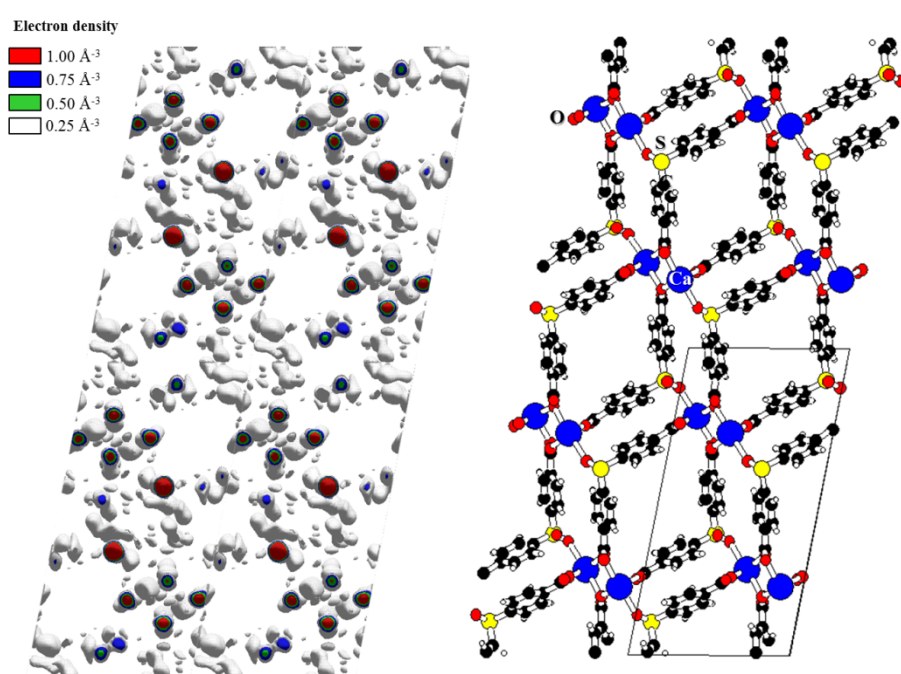
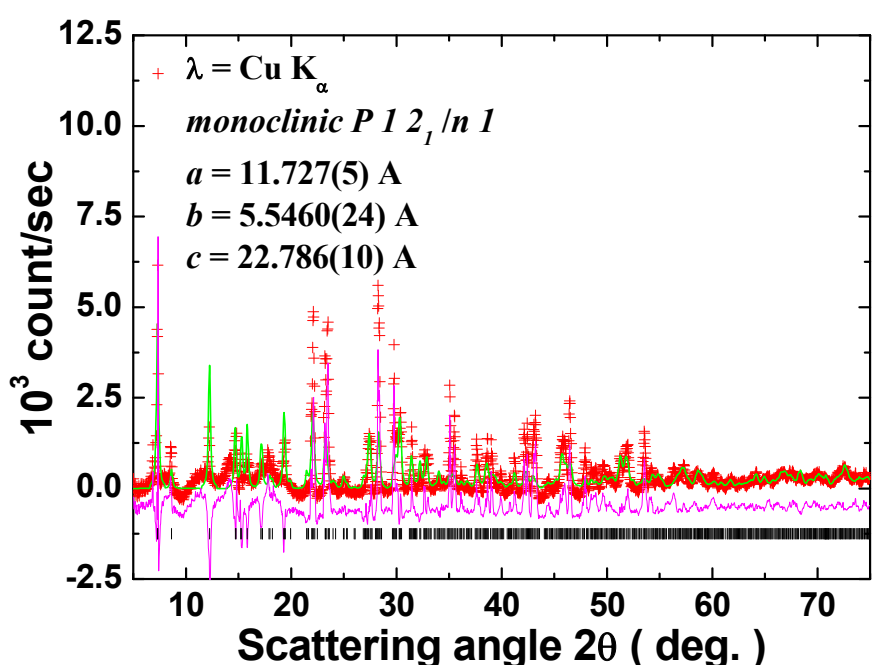


Figure S3. Observed (crosses) and fitted (solid lines) X-ray powder diffraction patterns for CYCU-1, assuming a monoclinic symmetry of space group  $P2_1/n$ . The difference between the calculated and observed is plotted at the bottom. The solid vertical lines mark the calculated positions of Bragg reflections for the proposed crystalline structure. The bottom plots are electron density from X-ray powder diffraction pattern and structure from single crystal X-ray diffraction.

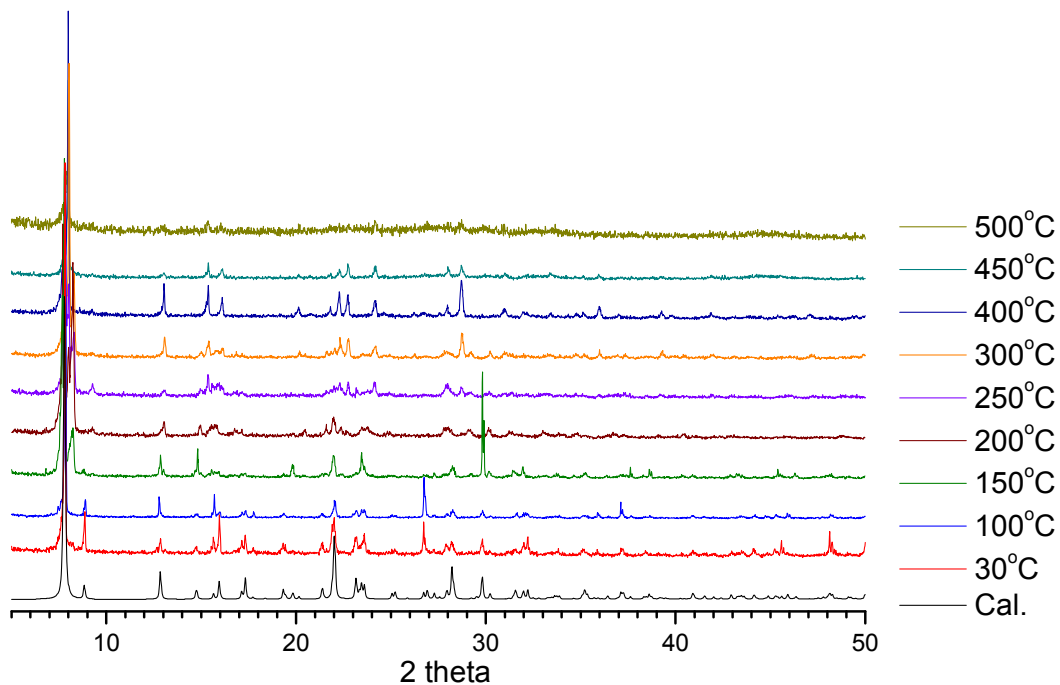


Figure S4. Powder X-ray diffraction patterns with varied temperatures for **CYCU-2**.

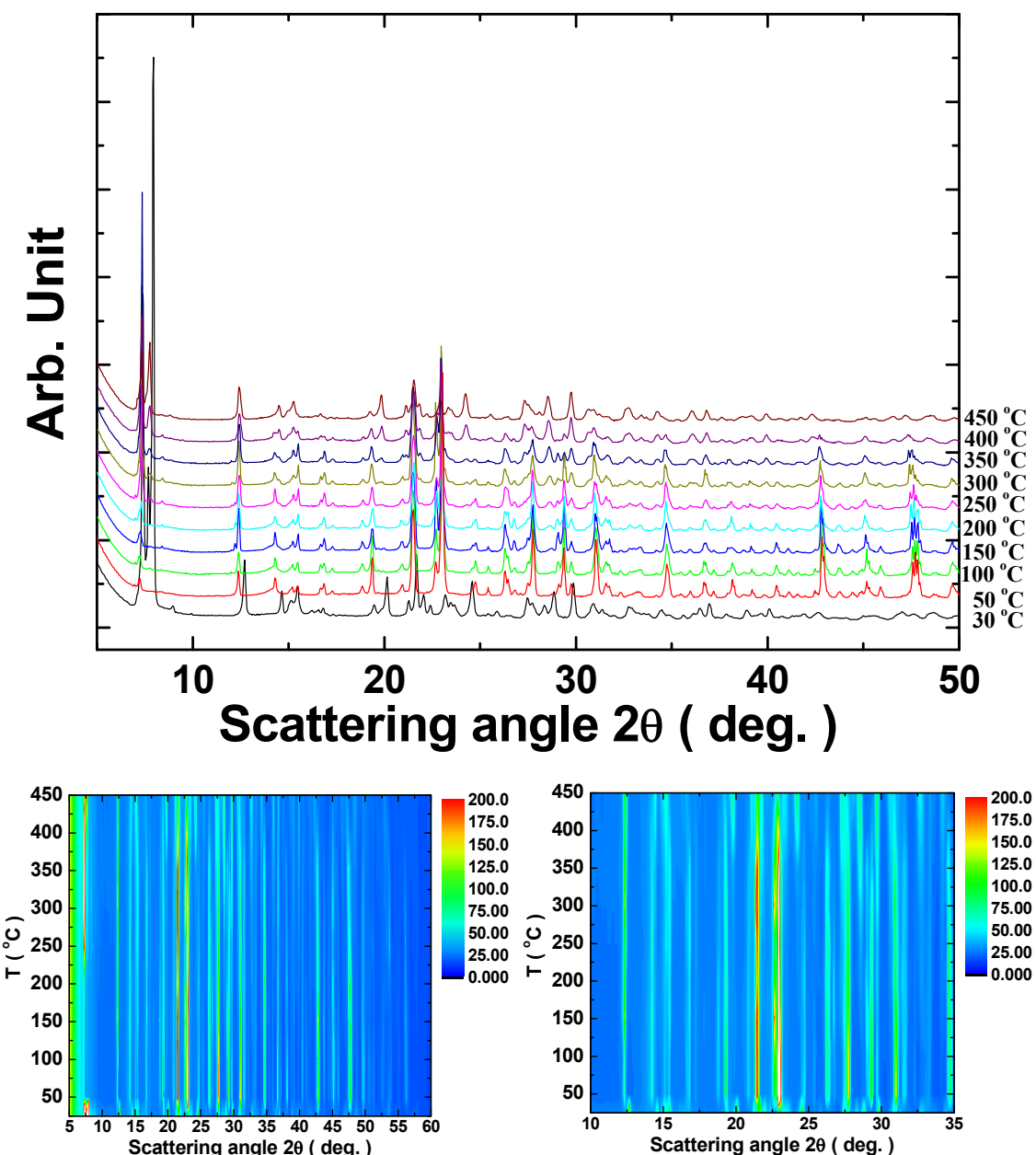


Figure S5. Powder X-ray diffraction patterns under vacuum ( $1 \times 10^{-4}$  torr) and varied temperatures for **CYCU-2**.

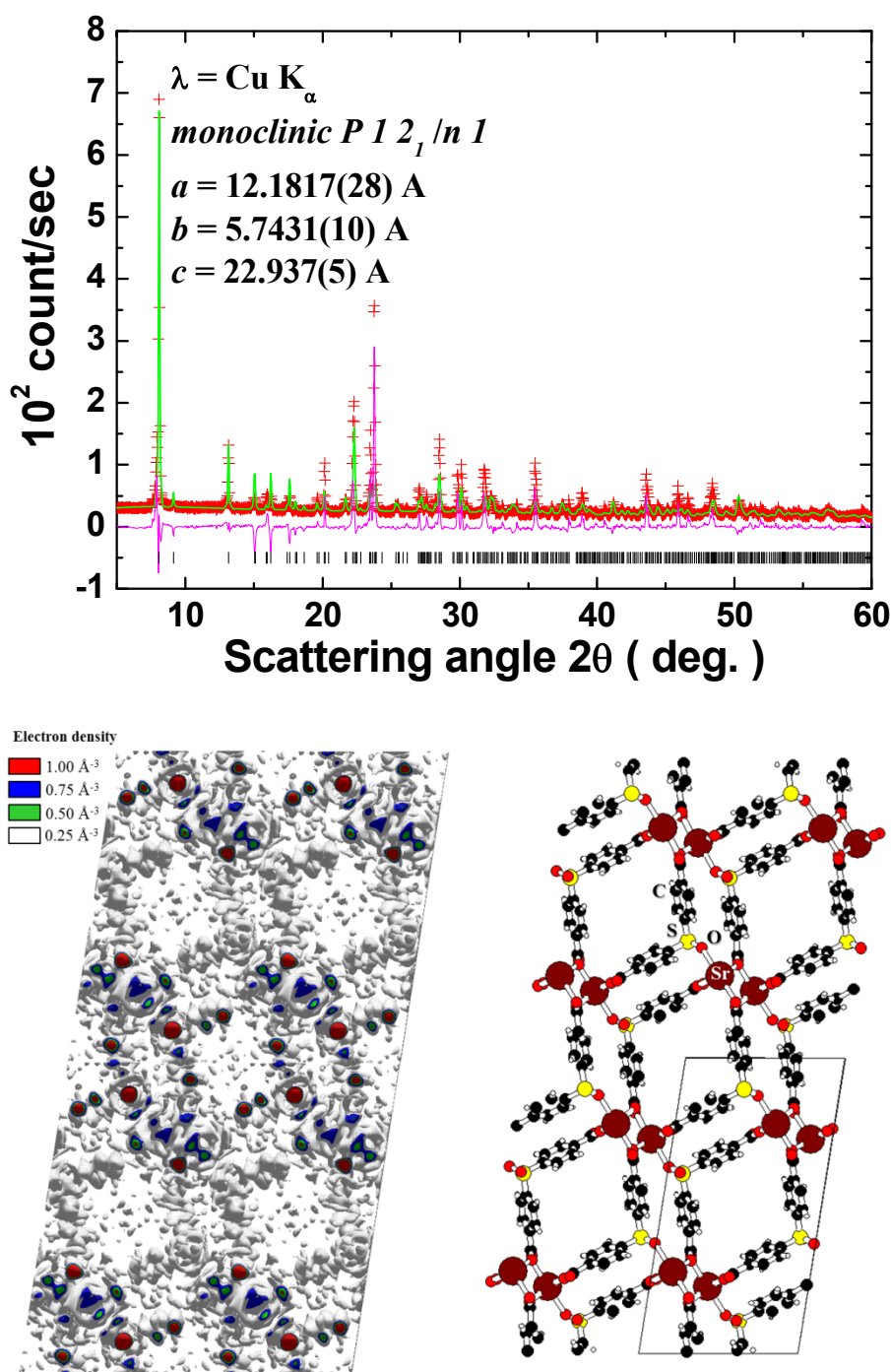
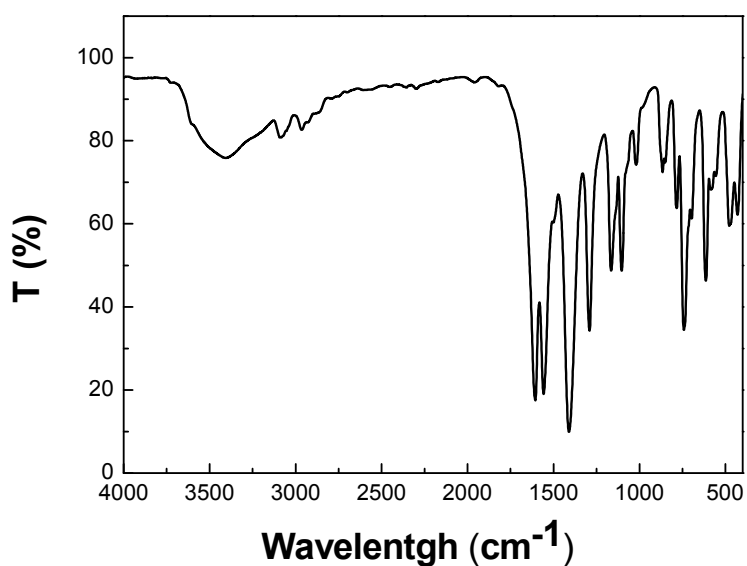


Figure S6. Observed (crosses) and fitted (solid lines) X-ray powder diffraction patterns for CYCU-2, assuming a monoclinic symmetry of space group  $P2_1/n$ . The difference between the calculated and observed is plotted at the bottom. The solid vertical lines mark the calculated positions of Bragg reflections for the proposed crystalline structure. The bottom plots are electron density from X-ray powder diffraction pattern and structure from single crystal X-ray diffraction.

(a) CYCU-1<sub>as</sub>



(b) CYCU-2<sub>as</sub>

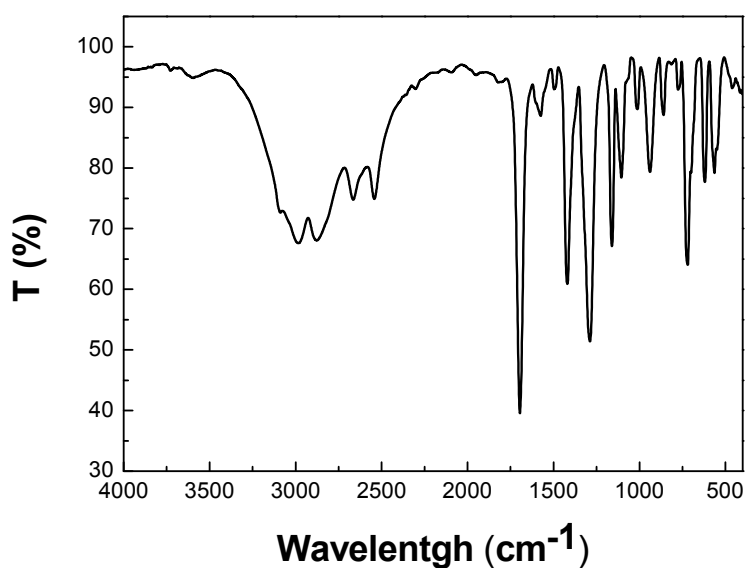
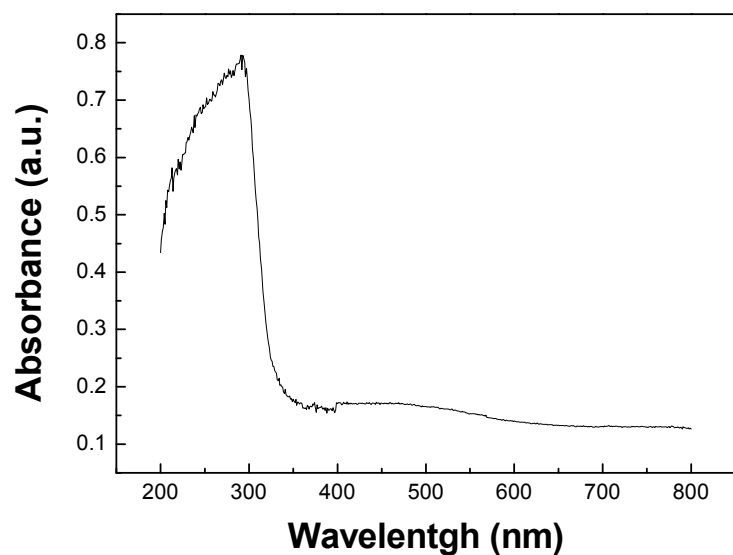


Figure S7. FT-IR spectra.

(a) CYCU-**1<sub>as</sub>**



(b) CYCU-**2<sub>as</sub>**

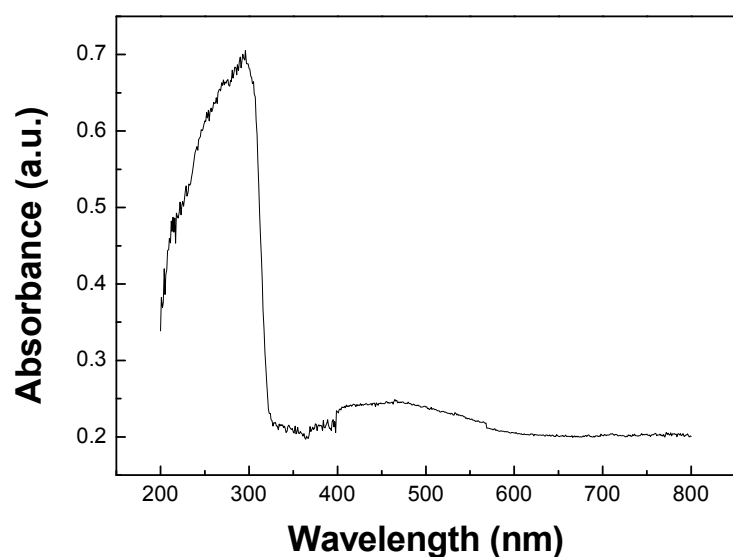
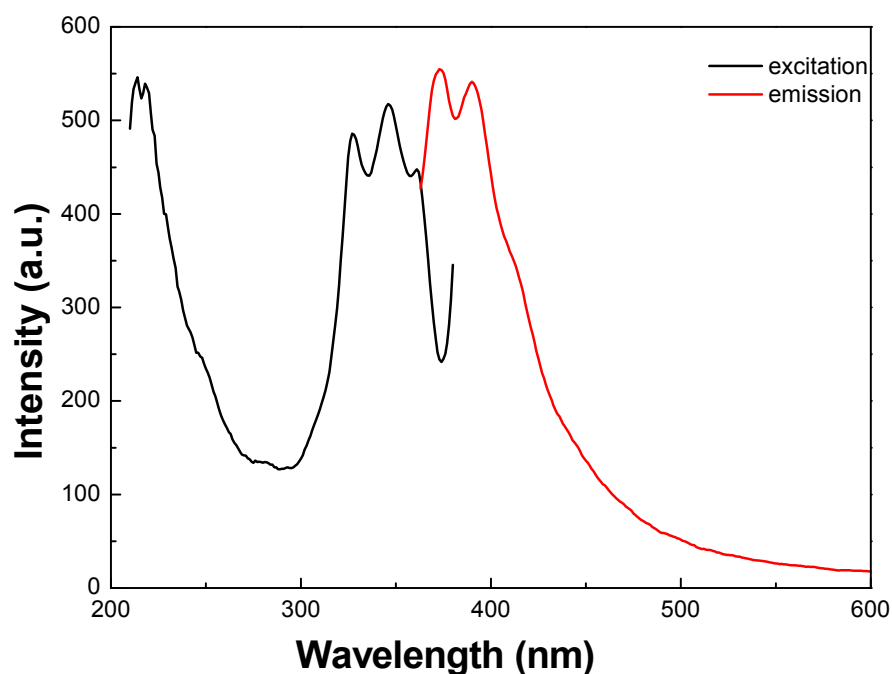


Figure S8. UV-vis absorption spectra.

(a) CYCU-1<sub>as</sub>



(b) CYCU-2<sub>as</sub>

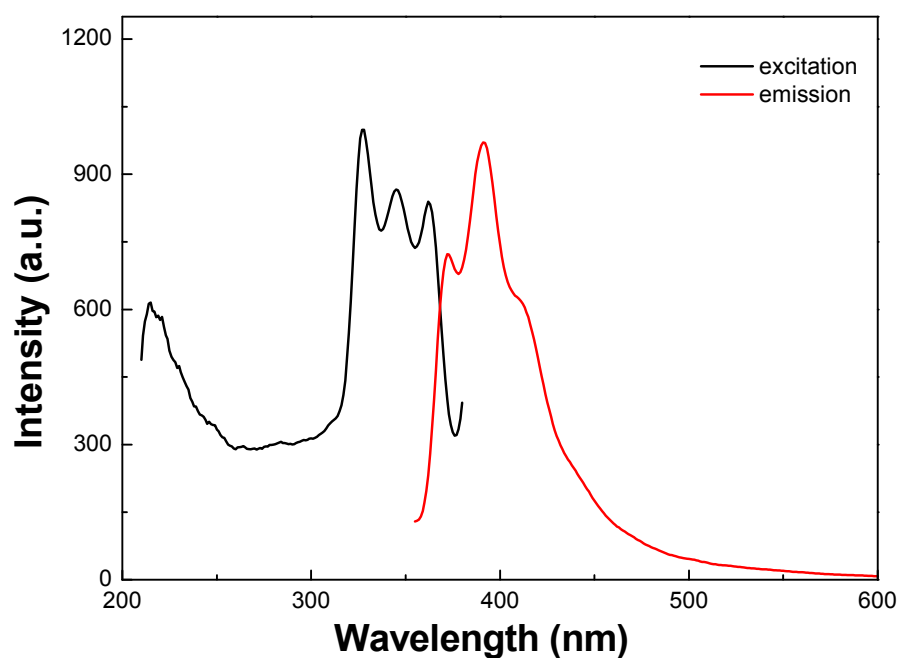
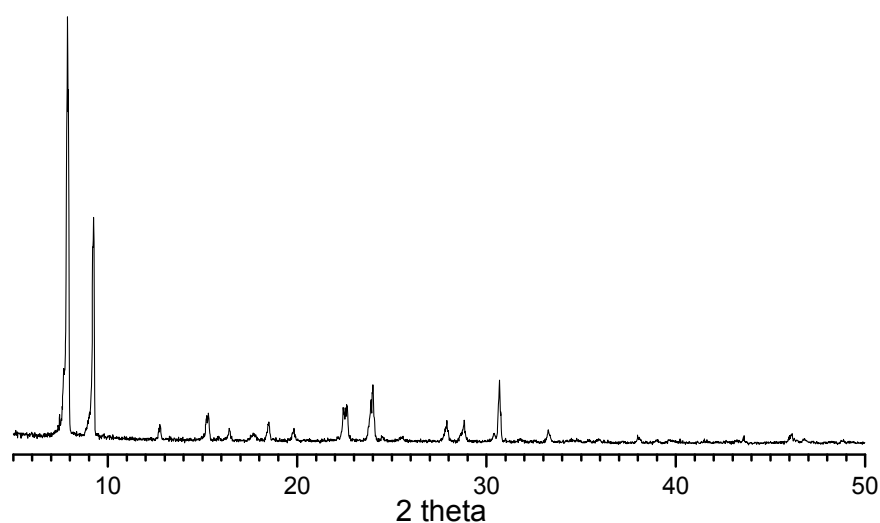


Figure S9. Photoluminescence emission spectra.

(a) CYCU-1



(a) CYCU-2

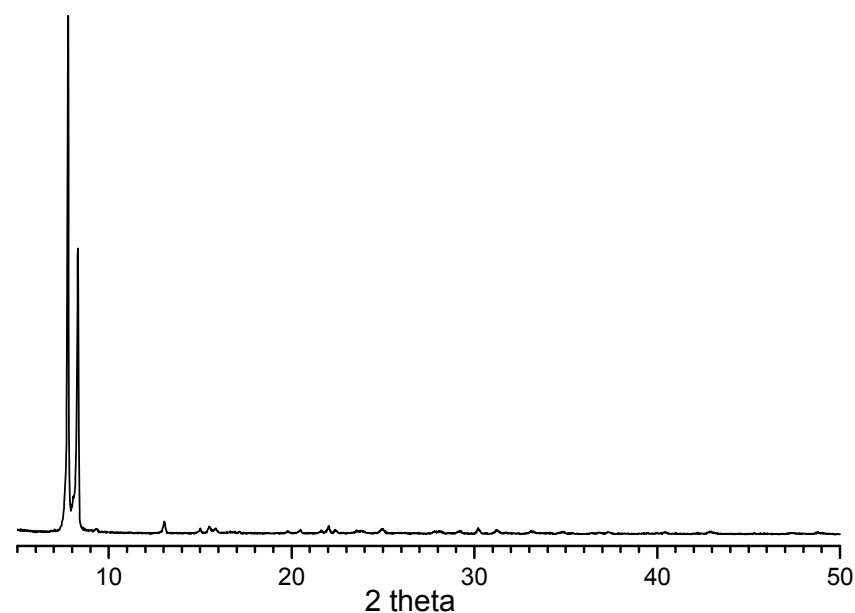
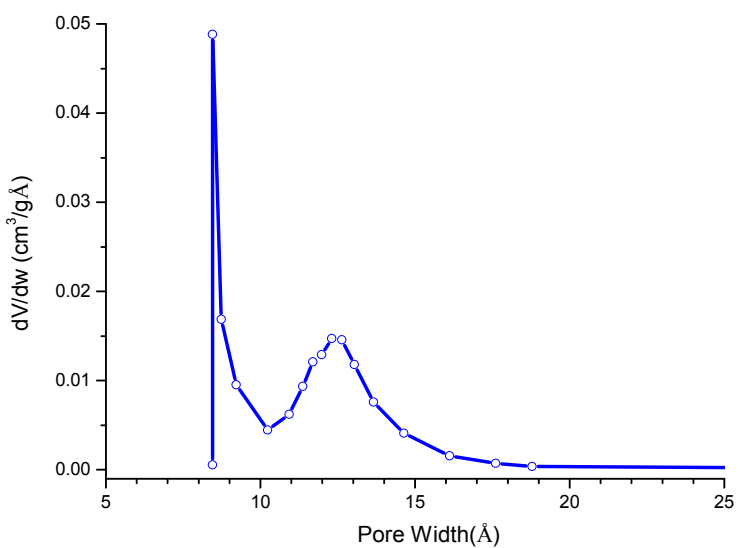


Figure S10. Powder X-ray diffraction patterns after N<sub>2</sub> sorption.

(a) CYCU-1



(a) CYCU-2

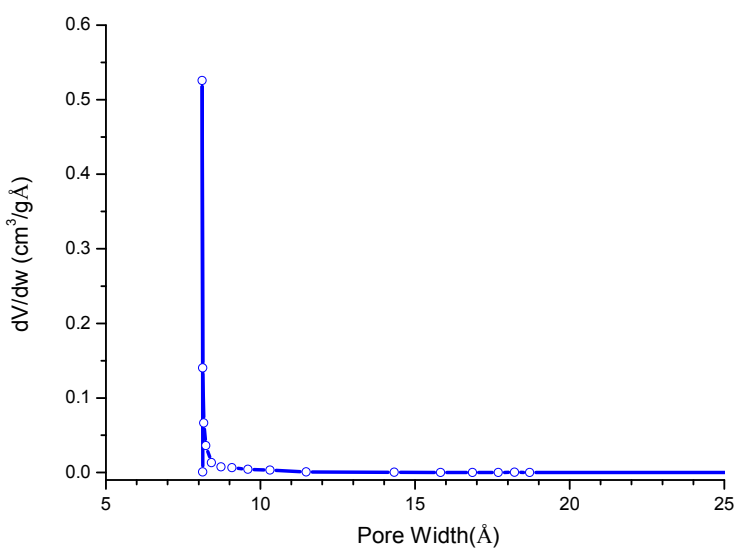


Figure S11. The pore size distributions obtained by the Horvath-Kawazoe (HK) method.

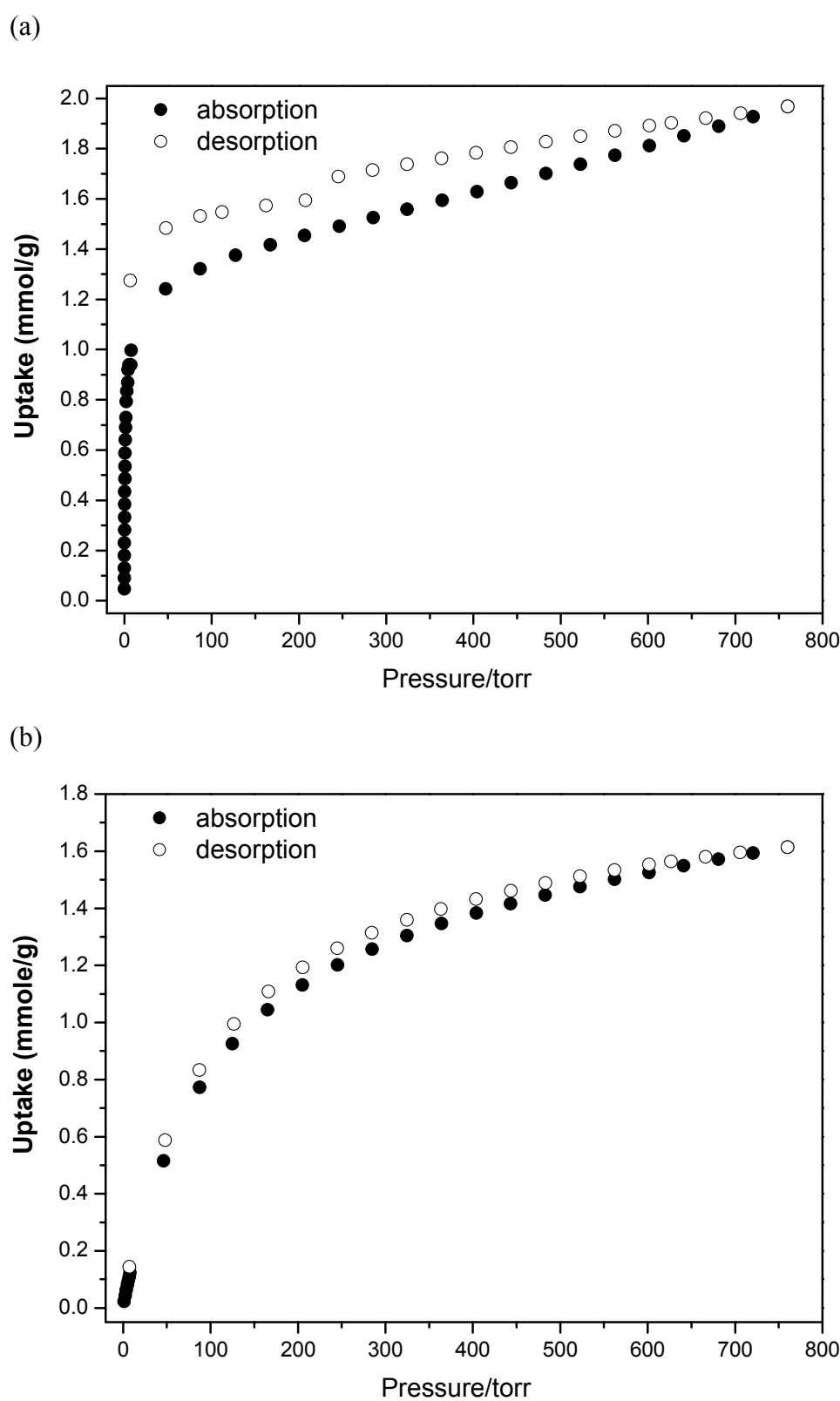


Figure S12. The CO<sub>2</sub> adsorption isotherms at (a) 195 K and (b) 273 K for **CYCU-1**.

### The isosteric heat of adsorption for hydrogen and carbon dioxide adsorption on CYCU-1.

The differential heat of adsorption was calculated from the measured carbon dioxide adsorption at 298 K and 273 K by applying the Clausius-Clapeyron equation:<sup>1</sup>

$$\frac{\Delta H_{iso}}{RT^2} = \left( \frac{\partial \ln P}{\partial T} \right)_n$$

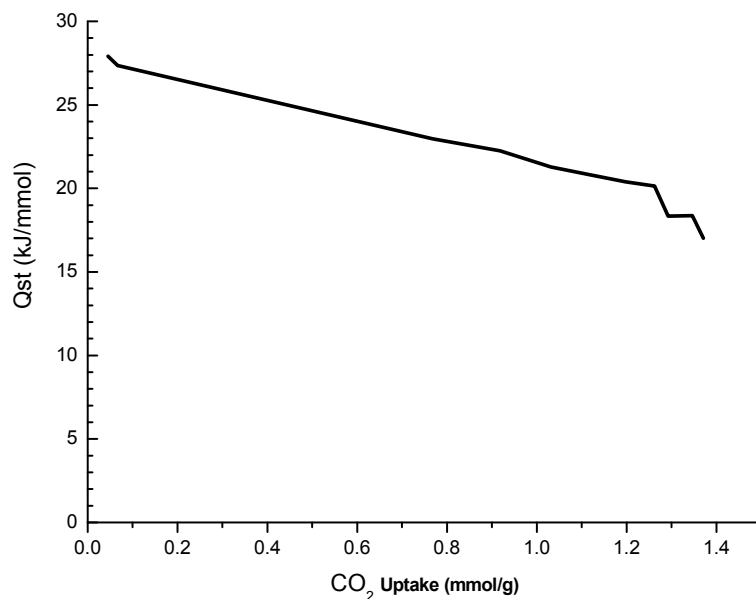


Figure S13. Isosteric heat of adsorption for  $\text{CO}_2$  in CYCU-1.<sup>1</sup>

**Table S1.** Selected bond lengths (Å).

CYCU-1 <sub>as</sub>			
Ca(1)-O(3)	2.2977(15)	Ca(1)-O(1)#1	2.4367(15)
Ca(1)-O(4)	2.3010(16)	Ca(1)-O(5)	2.4555(14)
Ca(1)-O(2)	2.3604(15)	Ca(1)-O(2)#2	2.8850(17)
Ca(1)-O(1)	2.3772(16)		
CYCU-1			
Ca(1)-O(3)#1	2.2868(17)	Ca(1)-O(1)#4	2.4324(17)
Ca(1)-O(4)#1	2.2873(18)	Ca(1)-O(5)	2.4475(17)
Ca(1)-O(2)#2	2.3439(16)	Ca(1)-O(2)#4	2.8870(18)
Ca(1)-O(1)#3	2.3678(17)		
CYCU-2 <sub>as</sub>			
Sr(1)-O(2)	2.4323(19)	Sr(1)-O(4)#1	2.5725(17)
Sr(1)-O(1)	2.4368(18)	Sr(1)-O(5)	2.5882(17)
Sr(1)-O(4)	2.4926(17)	Sr(1)-O(3)#2	2.9326(18)
Sr(1)-O(3)	2.5164(17)		
CYCU-2			
Sr(1)-O(2)	2.431(2)	Sr(1)-O(4)#1	2.573(2)
Sr(1)-O(1)	2.435(2)	Sr(1)-O(5)	2.589(2)
Sr(1)-O(4)	2.491(2)	Sr(1)-O(3)#2	2.937(2)
Sr(1)-O(3)	2.513(2)		

Symmetry transformations used to generate equivalent atoms: for CYCU-1<sub>as</sub>, #1

-x+1/2,y+1/2,-z+1/2, #2 -x+1/2,y-1/2,-z+1/2; for CYCU-1, #1 -x-1/2,y-1/2,-z+1/2, #2

-x,-y+2,-z, #3 -x,-y+1,-z, #4 x+1/2,-y+3/2,z+1/2; for CYCU-2<sub>as</sub> and CYCU-2, #1

-x+1/2,y-1/2,-z+3/2, #2 -x+1/2,y+1/2,-z+3/2.

## References

- S1. P. A. Webb, C. Orr, *Analytical Methods in Fine Particle Technology*; Micromeritics Instrument Corp.: Norcross, USA, 1997; pp 230-231.